

EFFECTS OF BAFFLE CONFIGURATIONS ON BIOMASS DISTRIBUTION IN ROTATING DRUM DRYER

*Yutthana SRIPA¹, Nuthvipa JAYRANAIWACHIRA¹ and Chinaruk THIANPONG¹

¹Department of Mechanical Engineering, King Mongkut's Institute of Technology Ladkrabang

¹Chalongkrung Road, Bangkok 10520, Thailand

Corresponding author: Yutthana SRIPA. E-mail: yutth_sri@yahoo.com

ABSTRACT

Rotating drum dryer commonly uses for removing moisture from drying granular or particulate solid. Drum drying performance greatly depends on convective heat transfer mechanism, that mostly involve the distribution characteristic of the particles over the drum. In this study, sawdust and shredded coconut distribution over the rotating drum cross section with various baffle configurations are presented. The two segments baffle of 120°, 135° and 150° were investigated with low and high moisture content, between 10% and 60%, of sawdust and shredded coconut. The rotating drum was made of stainless steel with inner diameter of 395 mm. The drum rotational speed was examined at 3, 4 and 5 rpm respectively. The particles hold-up and falling length were estimated by ImageJ programming, which analysed multiple photographs of the rotating drum cross section area at different experimental conditions. The particles volume ratio and falling length ratio were studied. It was found that the low moisture content shredded coconut with two segments baffle of 120° had significantly higher uniform distribution at any baffle angles and the drum rotational speeds. It was also found that the high moisture content sawdust with two segments baffle of 150° had significantly lower uniform distribution at any baffle angles with the drum rotational speed of 3 rpm. The experimental results were compared with theoretical calculation which reasonable agreement was obtained in comparison between them.

Keywords: Rotating drum dryer; Particles hold-up; Volume ratio; Falling length ratio

INTRODUCTION

Rotating or rotary drum dryers are used throughout the moisture removing from drying granular or particulate solid in various industries, such as foods industry, chemical industry, agricultural drying process and biomass drying for renewable energy production process, etc. The working principle of rotating drum drying is the removal of water from drying materials by supplying hot gas into the horizontal rotating drum, which fitted the baffles around the inside wall of the drum to hold up and strew the particles. The performance of rotating drum dryer greatly depends on convective heat transfer mechanism, which mostly involves the distribution characteristic of the particles over the drum. The design and specify of shape of baffle configurations for the different type of materials affects the distribution of particles over the drum. There are several studies reports about the design of baffles or flights in rotary drum dryer. The theoretical calculation of solids hold up in

flights with three segments, which provided estimates of the flight hold up was developed by D. Revolant et. al, [1]. The study of the performance of a rotary dryer in relation to number of flights was presented by M.H. Lisboa et. al, [2] the equations to calculate the area of the solids within two-segment flights and length of fall at any angle between the segments were determined. M.E. Sheehan et. al, [3] presented the amount of solids contained within the flights and in the airborne phase with image analysis techniques. The propose of the study was to estimate the cross-sectional area of material during the flights. In this study, the high and low moisture content biomass from agricultural product, with different sticky characteristics of the particles, were investigated over the distribution on the rotating drum with various baffle configurations.

EXPERIMENTAL SET-UP AND METHOD

Experimental set-up

The experimental study was carried out on a horizontal pilot rotating drum, which was made of seamless stainless steel at 5 mm thickness, 180mm in length and 395mm in inner diameter. The front cross section area of the drum was covered by transparent acrylic sheet at 4 mm thickness. The inside wall of the drum was equipped with removable baffles, which were also made of stainless steel at 2 mm thickness. Two segments baffle with angle of 120°, 135° and 150° between segments were used for comparison. The electric motor 1 HP with 60:1 gear ratio and NSP series inverter were used for driving the rotating drum and control the drum revolution speed at various experimental conditions. The experimental set up, the cross section of the drum and baffle arrangement are shown in fig 1 whereas the baffle configurations and dimensions were described in table 1 and fig 2, respectively. The DSLR camera Nikon D5300 (AF-S DX Nikkor 18-105mm f/3.5-5.6G ED VR lens) was used for video recording over the cross section of the drum with the full HD 1080p 60fps video format.



Fig.1 The rotating drum test set, shown the cross section of the drum and baffle arrangement.

Table 1 Configuration of the baffles.

Parameter	α , °	L ₁ , mm	L ₂ , mm	No. of baffle
Type 1	120	40	20	12
Type 2	135	30	30	12
Type 3	150	30	25	12

*The three types of the baffles were kept equal Ro.

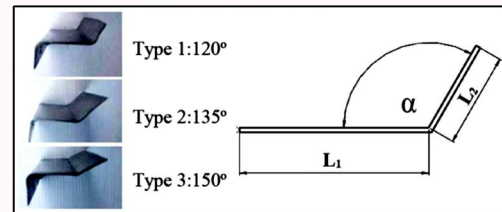


Fig. 2 The baffle dimensions.

MATERIALS

Biomass particles, sawdust and shredded coconut were used as experimental material. Sawdust used in this study was obtained from sawmill factory, located in Chonburi province while shredded coconut was obtained from coconut oil press factory located in Ratchaburi province, Thailand. The moisture content of sawdust was around 50% (w.b.). The moisture content shredded coconut was high around 60% (w.b.), whereas the low moisture content shredded coconut was around 10% (w.b.).

EXPERIMENTAL METHOD

To study the distribution characteristic of the biomass particles over the drum, first the pilot rotating drum was set in horizontal arrangement with 1.2 m from ground to the center of the drum. The 12 removable baffles of each type were fitted on the inner wall of the drum at every 30 degree on the perimeter of the drum in counter-clockwise direction. The particles, fed into the drum, were at 15% of the total volume of the drum. The drum rotational speeds were adjusted by NSP series inverter at 3, 4 and 5 rpm, respectively. The dynamic angle of repose of particles was examined by rotating the drum with the particles inside but without the baffles, as shown in fig 3. The experimental conditions were shown in table 2. The DSLR camera was attached on the tripod, which aligned at the drum center at 2.5 m distance.



Fig.3 The investigation of the dynamic angle of repose of shredded coconut with the drum rotational speed at 4 rpm.

Table 2 Experimental conditions.

Parameter	Value
Drum rotational speed(rpm)	3/4/5
Particle volume	15 % (by drum volume)
Moisture content of particle	
- Sawdust	50 % (w.b.)
- Shredded coconut	60 % and 10 % (w.b.)

The particles flow behavior over the cross section of the drum at any baffle angle(θ) were taken by the DSLR camera Nikon D5300 in the full HD 1080p 60 fps video formats as shown in fig 4.



Fig.4 The particles distribution over the cross section of the drum was taken by the DSLR camera Nikon D5300.

ANALYSYS

In this study, the effects on the particle distribution of biomass in the rotating drum were investigated by photograph analysis. The photographs were captured from the rotating drum cross section video at different baffle angles. The hold-up(the area of particles within the baffles) and falling length(the distance from the edge of the baffle to the particles at the bottom of the drum) were estimated by ImageJ computer software programming. The manual process ImageJ, which set the scaling process for defining the length of pixel(the diameter of the drum)was used for computing the frontal area of particles within the baffles and the falling length at various experimental conditions. The example of the enclosed area of the particles within the baffle, which was computed by ImageJ software program, was shown in fig 5.

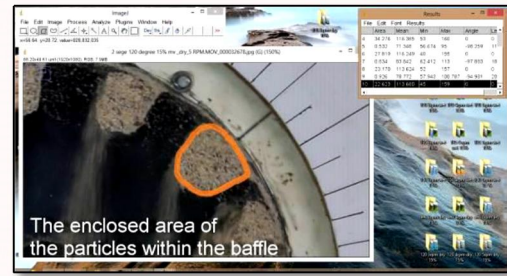


Fig.5 The enclosed area of the particles within the baffle was computed by ImageJ software program.

The volume ratio(VR) and the falling length ratio(FR) were presented to describe the distribution behavior of the biomass particles over the cross section of the drum in this study, which indicated the tendency of decreasing rate of the particles volume within the baffles at higher baffle angle. The experimental results were compared with theoretical calculation, which calculated the section area occupied by the particles within the baffles and falling length from the equations. The theoretical calculation of the cross section area occupied by particles within the baffles according to the set of equations of D. Revol et. al, [1]and M.H. Lisboa et. al, [2] as follow :

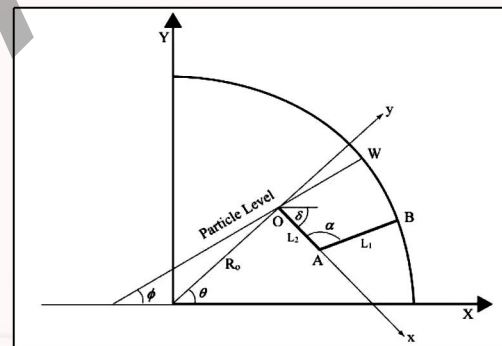


Fig.6 The cross section of two segments baffle.

From Fig.6, the coordinate of segments, $L_1 : (y_1 = 0)$,

$L_2 : (y_2 = a_2 + b_2 x)$ with $a_2 = x_A \tan(\alpha)$ and $b_2 = -\tan(\alpha)$

The coordinate of points, A : $x_A = L_2$ and $y_A = 0$

B : $x_B = x_A - L_1 \cos(\alpha)$ and $y_B = L_1 \sin(\alpha)$

Since point B was located on the wall of the drum, then

$$x_B^2 + y_B^2 = R^2 \quad \dots(1)$$

The two sets of coordinate,

$$\begin{aligned} X_B &= X_o + x_B \cos(\delta) - y_B \sin(\delta) \\ R_o \cos(\theta) + x_B \cos(\delta) - y_B \sin(\delta) & \dots(2) \end{aligned}$$

$$\begin{aligned} Y_B &= Y_o + y_B \cos(\delta) - x_B \sin(\delta) \\ R_o \sin(\theta) + y_B \cos(\delta) - x_B \sin(\delta) & \dots(3) \end{aligned}$$

Substituting Equation (2) and (3) into Equation (1), for solving δ at any baffle angle position(θ). The equation for the particle level line is given by

$$y = x \tan(\gamma) = x \tan(\phi - \delta) \dots(4)$$

The intersection of the line tracing the second segment is determined by the following equation.

$$x_2 = \frac{a_2}{\tan(\gamma) - b_2} \dots(5)$$

$$y_2 = a_2 + b_2 x_2 \dots(6)$$

The intersection of the particle level line with the drum wall is calculated by the following equation.

$$x_w = -\frac{B_w \pm \sqrt{B_w^2 - 4A_w C_w}}{2A_w} \dots(7)$$

With $A_w = 1 + [\tan(\gamma)]^2$,

$$B_w = 2X_o [\cos(\alpha) - \tan(\gamma)\sin(\delta)] + 2Y_o [\tan(\gamma)\cos(\delta) + \sin(\alpha)]$$

$$C_w = R_o^2 - R^2$$

Three types of particle fills can occur :

- 1) The particles reach the drum wall.

If $\gamma > \arctan\left(\frac{y_B}{x_B}\right)$ since the section area occupied by the particles is given by

$$S = \frac{R^2}{2} [\beta - \sin(\beta)] + \frac{1}{2} |x_A y_A - x_B y_A + x_B y_w - x_w y_B| \dots(8)$$

$$\text{With } \beta = 2\sin^{-1} \left[\frac{\sqrt{(x_B - x_w)^2 + (y_B - y_w)^2}}{2R} \right]$$

- 2) The particles do not reach the wall, but reach the second segment.

$$\text{If } \gamma < \arctan\left(\frac{y_B}{x_B}\right), \sqrt{(x_2 - x_A)^2 + (y_2 - y_A)^2} < L_2 \text{ and } y_2 > 0,$$

since the area of the transversal section occupied by the material was given by

$$S = \frac{1}{2} |x_A y_2| \dots(9)$$

3) The particles do not remain within the baffle. If $y_2 < 0$ The falling length theoretical calculation at any baffle angle positions according to the equations of M.H. Lisboa et. al, [2], which determined the falling length is the straight-line distance of the particles from the edge of the flight to the particles bed in the lower part of the drum.

$$Y_d = \frac{Y_o + \sqrt{R^2 - X_o^2}}{\cos \alpha} \dots(10)$$

With $Y_o = R_o \sin \theta$ and $X_o = R_o \cos \theta$

The volume ratio (VR) and the falling length ratio (FR) were applied from the section area occupied by the particles within the baffles (S) and the falling length (Yd), which were calculated by the set of equations of D. Revol and et. al, [1] and M.H. Lisboa and et. al, [2].

$$VR = \frac{V_i}{V_o} \dots(11)$$

with $V = S \times L$

$$FR = \frac{Y_{dr}}{R} \dots(12)$$

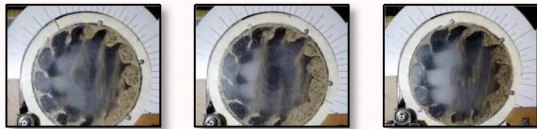
RESULTS

The effects on the distribution of the biomass particles in the pilot rotating drum with 3 different types of baffles were investigated by video capture photographs analysis, which were estimated the area of particles within the baffles and the falling length using ImageJ computer software program. The video capture photographs of low and high moisture content shredded coconut and sawdust over the cross section of the drum, rotated at 5 rpm, were shown in fig 7, 8 and 9, respectively.



120° 135° 150°

Fig. 7 The video capture photographs of low moisture-content shredded coconut over the cross section of the drum.(from left to right, baffle type 1 with $\alpha = 120^\circ$, type 2 with $\alpha = 135^\circ$ and type 3 with $\alpha = 150^\circ$)



120° 135° 150°

Fig. 8 The video capture photographs of high moisture content shredded coconut over the cross section of the drum.(from left to right, baffle type 1 with $\alpha = 120^\circ$, type 2 with $\alpha = 135^\circ$ and type 3 with $\alpha = 150^\circ$)



120° 135° 150°

Fig. 9 The video capture photographs of high moisture content sawdust over the cross section of the drum.(from left to right, baffle type 1 with $\alpha = 120^\circ$, type 2 with $\alpha = 135^\circ$ and type 3 with $\alpha = 150^\circ$)

In this study, the volume ratio (VR) and the falling length ratio (FR) were presented to describe the distribution behavior of the high moisture content of sawdust and shredded coconut over the cross section of the drum. In the case of low moisture content shredded coconut, the results of the volume ratio of particles within the baffles type 1, 2 and 3 at the different baffle angle position shown in fig. 10, fig. 11 and fig. 12, respectively.

From fig. 10, it was found that the volume ratio decreased with the increase of baffles angle. The particles did not remain within the baffles at the baffle angle of 120° for all rotational drum speeds. The volume ratio from calculation were significantly lower than those from the experiment at the baffle angle of 50° to 100° and the volume ratio rapidly decreased from 100° to 110° . This can be attributed that the cohesive characteristic of moist shredded coconut caused the uncertain falling behaviour.

As shown in fig. 11, the average decreasing rate of the volume ratio at 3, 4 and 5 rotational

drum speeds were 0.073, 0.081 and 0.079, respectively. It can be described that the particles volume decreased 7.3%, 8.1% and 7.9% at every 10° of baffle angle when compared with the particles volume at the baffle angle positions at 0° . The particles were not hold within the baffles at the baffle angle of 110° .

As shown in fig. 12, the decreasing of the volume ratio is more uncertain than those of the baffle type 1, $\alpha = 120^\circ$ and type 2 $\alpha = 135^\circ$ (fig. 10 and 11). The particles were not hold within the baffles at the baffle angle of 100° .

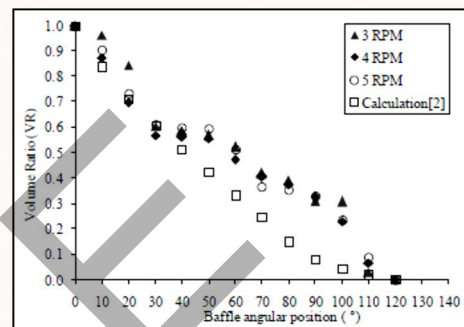


Fig.10 Effects of baffle type 1:120o and rotational speeds of the drum on the volume ratio of low moisture content shredded coconut at different baffle angle positions.

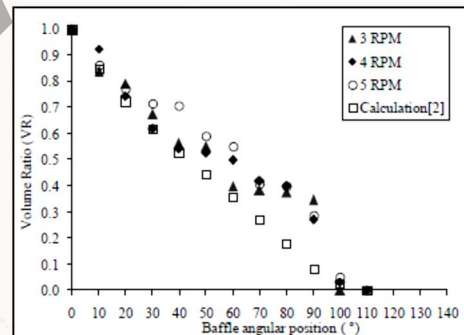


Fig. 11 Effects of baffle type 2:135o and rotational speeds of the drum on the volume ratio of low moisture content shredded coconut at different baffle angle positions.

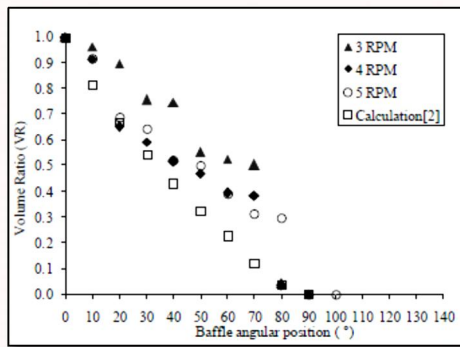


Fig. 12 Effects of baffle type 3:150o and rotational speeds of the drum on the volume ratio of low moisture content shredded coconut at different baffle angle positions.

Fig 13, 14 and 15 show the falling length ratio of low moisture content shredded coconut at different baffle angle. From these figures, the falling length ratio increased during the baffles angle increased until it reached the maximum value at the baffle angle of 90o. The falling length ratio decreased after the baffle angle passed 90o. As shown in fig. 15, the maximum falling length ratio at the drum rotational speeds of 3 rpm, 4 rpm and 5 rpm were 0.89, 0.90 and 0.89, respectively. It can be described that the maximum falling length were 89%, 90% and 89% when compared with the drum radius.

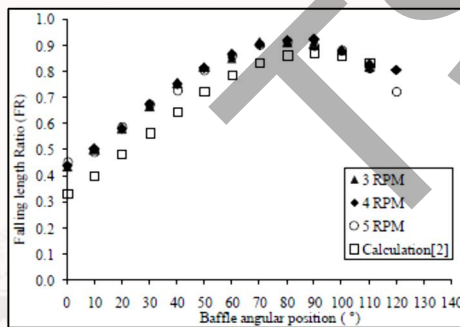


Fig. 13 Effects of baffle type 1:120o and rotational speeds of the drum on the falling length ratio of low moisture content shredded coconut at different baffle angle positions.

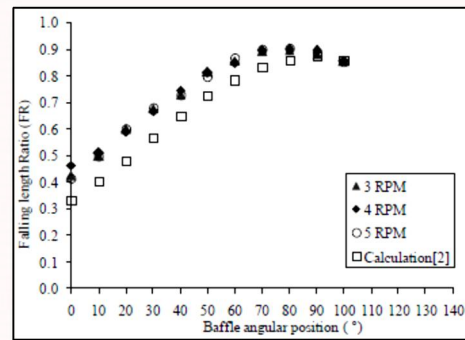


Fig. 14 Effects of baffle type 2:135o and rotational speeds of the drum on the falling length ratio of low moisture content shredded coconut at different baffle angle positions.

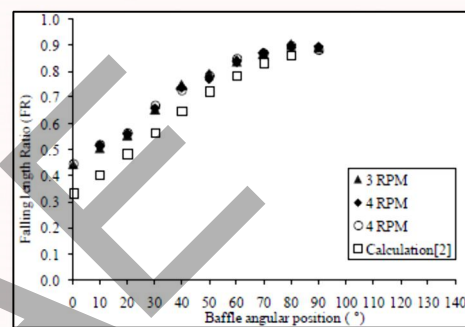


Fig. 15 Effects of baffle type 3:150o and rotational speeds of the drum on the falling length ratio of low moisture content shredded coconut at different baffle angle positions.

Fig. 16, 17 and 18 show the volume ratio of particles within the baffles type 1, 2 and 3 at the different baffle angle in the case of high moisture content shredded coconut.

As shown in fig.16, the average decreasing rate of the volume ratio of the baffle type 1:120o at the drum rotational speeds of 3 rpm, 4 rpm and 5 rpm were 0.075, 0.078 and 0.077, respectively. The volume ratio from calculation were significantly lower than those from the experiment at the baffle angle of 60° to 110°. This can be attributed that the sticky characteristic of high moisture content shredded coconut caused the uncertain falling behaviour.

From fig. 17, the particles were not hold within the baffles at the baffle angle of 110°. The average decreasing rate of the volume ratio at 3, 4 and 5 rotational drum speeds were 0.090, 0.100 and 0.092, respectively. It can be described that the particles volume decreased 9.09%, 10.00% and 9.23% at every 10° of baffle angle when compared with the particles volume at the baffle angle positions at 0°. As shown in fig. 18, The volume ratio from

calculation were significantly lower than those from the experiment at the baffle angle of 50° to 70°.

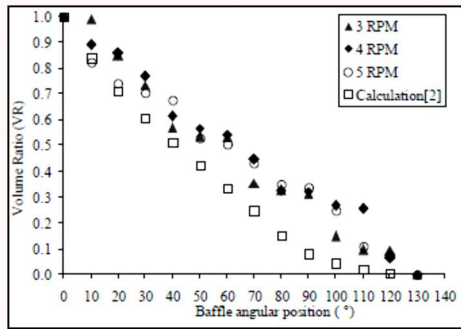


Fig. 16 Effects of baffle type 1:120° and rotational speeds of the drum on the volume ratio of high moisture content shredded coconut at different baffle angle positions.

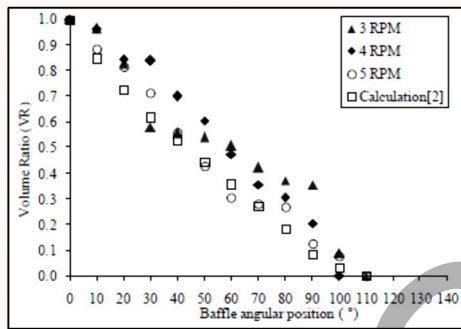


Fig. 17 Effects of baffle type 2:135° and rotational speeds of the drum on the volume ratio of high moisture content shredded coconut at different baffle angle positions.

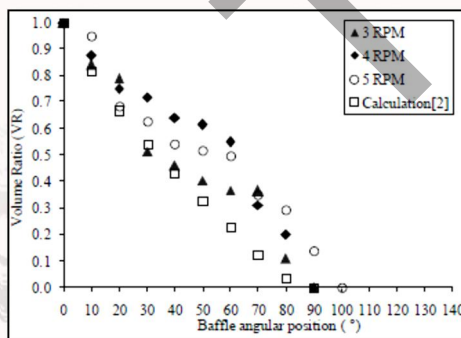


Fig. 18 Effects of baffle type 3:150° and rotational speeds of the drum on the volume ratio of high moisture content shredded coconut at different baffle angle positions.

As shown in fig. 20, the maximum falling length ratio at the drum rotational speeds of 3 rpm, 4 rpm and 5 rpm were 0.90, 0.90 and 0.91 at the baffle angle of 90°.

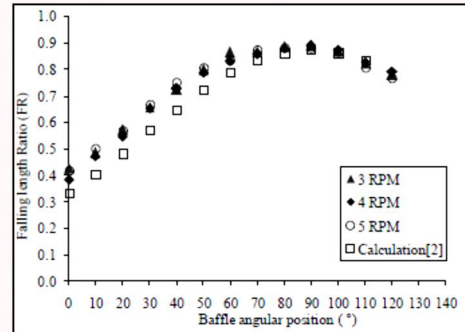


Fig. 19 Effects of baffle type 1:120° and rotational speeds of the drum on the falling length ratio of high moisture content shredded coconut at different baffle angle positions.

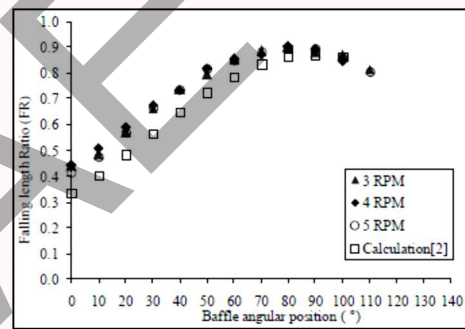


Fig. 20 Effects of baffle type 2:135° and rotational speeds of the drum on the falling length ratio of high moisture content shredded coconut at different baffle angle positions.

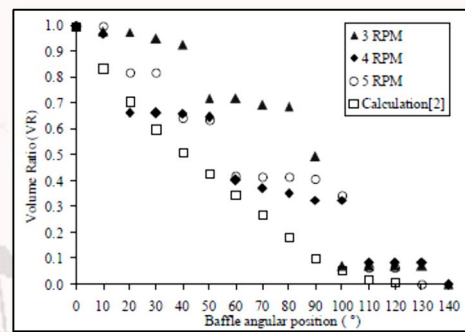


Fig. 22 Effects of baffle type 1:120° and rotational speeds of the drum on the volume ratio of high moisture content sawdust at different baffle angle positions.

Fig. 19, 20 and 21 show the falling length ratio of high moisture content shredded coconut at different baffle angle. The falling length ratio increased during the baffle angle increased until it reached the maximum value at the baffle angle of 90° similarly with the previous cases.

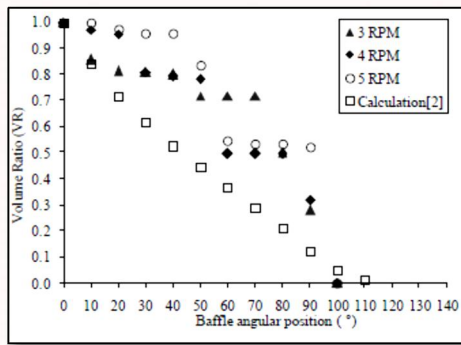


Fig. 23 Effects of baffle type 2:135° and rotational speeds of the drum on the volume ratio of high moisture content sawdust at different baffle angle positions.

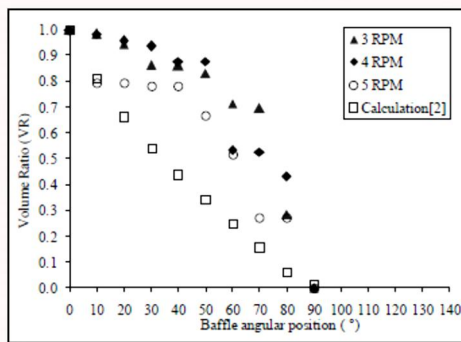


Fig. 24 Effects of baffle type 3:150° and rotational speeds of the drum on the volume ratio of high moisture content sawdust at different baffle angle positions.

Fig. 22, 23 and 24 show the volume ratio of high moisture content sawdust particles within the baffles type 1, 2 and 3 at the different baffle angle. From fig. 22, it was found that the volume ratio decreased non-uniformly at all of the rotational drum speeds. At 3 rpm of rotational drum speed, the volume ratio slowly decreased between the baffle angle of 10° to 40°, 50° to 80° and 100° to 130°, whereas rapidly decreased from 90° to 100°. This can be attributed that the cohesive

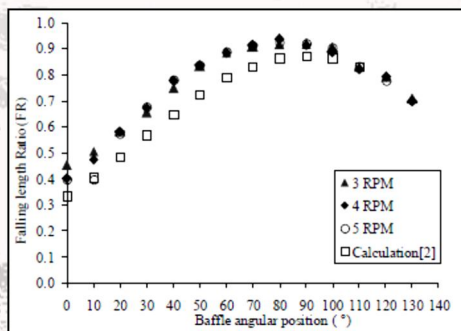


Fig. 25 Effects of baffle type 1:120° and rotational speeds of the drum on the falling length ratio of high moisture content sawdust at different baffle angle positions. characteristic of high

mois-ture content sawdust caused the uncertain fall-ing behaviour.

Fig. 25, 26 and 27 show the falling length ratio of high moisture content sawdust at different baffle angle. The falling length ratio increa-sedduring the baffles angle increased until it reached the maximum value at the baffle angle of 90° and decreased after the baffle angle passed 90° similarly with the other cases. As shown in fig. 25, the maximum falling length ratio at the drum rotational speeds of 3 rpm, 4 rpm and 5 rpm were 0.92, 0.91 and 0.92, respectively. It can be described that the maximum falling length were 92%, 91% and 92% when compared with the drum radius.

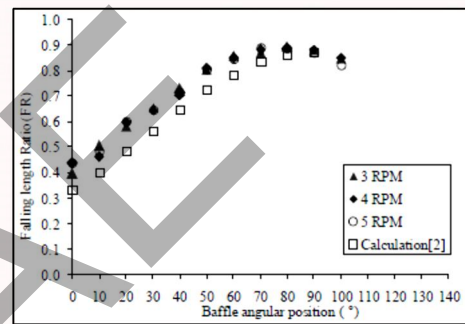


Fig. 26 Effects of baffle type 2:135° and rotational speeds of the drum on the falling length ratio of high moisture content sawdust at different baffle angle positions.

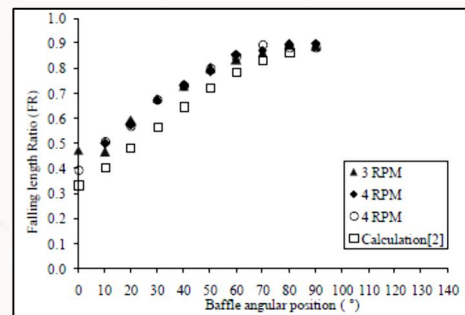


Fig. 27 Effects of baffle type 3:150° and rotational speeds of the drum on the falling length ratio of high moisture content sawdust at different baffle angle positions.

CONCLUSIONS

The results of the experiments shown the distribution characteristics of particles, which were visually investigated of the flow behavior over the cross section of the drum. The volume ratio of particles within the baffle and the falling length ratio at any baffle angles at different rotational speeds of the drum were presented. It was found that the cohesive

characteristic of the moist biomass particles caused the material to be non uniform distribution which were clearly shown in fig 22, 23 and 24. The non uniform distribution would make the unsteady reduction of retained volume on the baffle when compared with the calculation. The clumped up material, due to high moisture content, such as sawdust was less airborne and failed as a lump.

In the case of various α , the decreasing of α caused more distribution period of the particles into the drum. From the experiments, it was found that the case of using baffle of 120° was the highest airborne distribution, which was due to the highest period of particles fall. It was found that the low moisture content shredded coconut with two segments baffle of 120° had significantly higher uniform distribution at any baffle angles and the drum rotational speeds. It was also found that the high moisture content sawdust with two segments baffle of 150° had significantly lower uniform distribution at any baffle angles with the drum rotational speed of 3 rpm.

The average of the falling length ratio from the experiments was higher than those of theoretical calculation because the free flow particles were slightly projectile when they were strew from the baffles. Therefore, the falling length, measured by ImageJ program, was longer than the calculation from equation (10) which concerned only the falling in vertical only.

The present study is in the initial stage, which could give the distribution behavior of moist sawdust and shredded coconut over the various baffle configurations for the efficiency enhancement of the rotating drum dryer in the further study.

NOMENCLATURE

L_1	length of first baffle segment (m)
L_2	length of second baffle segment (m)
y_1	coordinate of the point of first baffle segment (m)
y_2	coordinate of the point of second baffle segment (m)
x_A, y_A	coordinate of the point A (m)
x_B, y_B	coordinate of the point B (m)
x_w, y_w	coordinate of the point W at the intersection of particle level with the wall (m)
α	angle between the first and second baffle segments (rad)
θ	the baffle angle position (rad)
\emptyset	dynamic angle of repose (rad) \square
R	drum radius (m)
R_o	radius of the circle traced by the baffle tip (m)

S	cross-sectional area of the particle within the baffle (m ²)
L	length of the drum (m)
V	volume of the particle within the baffle (m ³)
V_i	volume of the particle within the baffle at any the baffle angle position (m ³)
V_o	volume of the particle within the baffle at the baffle angle of 0° (m ³)
w.b.	wet basis moisture content (%)
Y_d	falling length (the distance of the particles from the edge of the baffle to the bottom bed of the drum) (m)
Y_{di}	falling length (the distance of the particles from the edge of the baffle to the bottom bed of the drum at any the baffle angle position) (m)
VR	volume ratio
FR	falling length ratio

REFERENCES

- [1] D. Revol, C.L. Briens and J.M. Cha-bagno. . The design of flights in rotary dry-ers. Research Journal of Powder Techno-logy. 121: 230-238 (2001)
- [2] M. H. Lisboa, D. S. Vitorino, W. B. Del-aiba, J. R. D. Finzer and M. A. S. Bar-rozo. A study of Particle Motion in Rotary Dryer. Brazilian Journal of Chemical Engi-neering. 24(03): 365-374 (2007)
- [3] O.O. Ajayi, M.E. Sheehan. Application of image analysis to determine design loading in fli-ghted rotary dryers. Powder Technology. 223: 123-130 (2012)